# Spatio-Temporal Analysis and Prediction of Cellular Traffic in Metropolis

Xu Wang*, Zimu Zhou†, Zheng Yang*, Yunhao Liu*, Chunyi Peng‡
*School of Software and TNList, Tsinghua University
†Computer Engineering and Networks Laboratory, ETH Zurich
‡Dept. CSE, The Ohio State University
xu-wang15@mails.thu.edu.cn, zzhou@tik.ee.ethz.ch, {yangzheng, yunhao}@tsinghua.edu.cn, chunyi@cse.ohio-state.edu

***Abstract*—Understanding and predicting cellular traffic at large-scale and fine-granularity is beneficial and valuable to mobile users, wireless carriers and city authorities. Predicting cellular traffic in modern metropolis is particularly challenging because of the tremendous temporal and spatial dynamics introduced by diverse user Internet behaviours and frequent user mobility citywide. In this paper, we characterize and investigate the root causes of such dynamics in cellular traffic through a big cellular usage dataset covering 1.5 million users and 5,929 cell towers in a major city of China. We reveal intensive spatio-temporal dependency even among distant cell towers, which is largely overlooked in previous works. To explicitly characterize and effectively model the spatio-temporal dependency of urban cellular traffic, we propose a novel decomposition of in-cell and inter-cell data traffic, and apply a graph-based deep learning approach to accurate cellular traffic prediction. Experimental results demonstrate that our method consistently outperforms the state-of-the-art time-series based approaches and we also show through an example study how the decomposition of cellular traffic can be used for event inference.**

## I. Introduction

With billions of mobile devices accessing the Internet via 3G/4G/5G networks, cellular traffic has skyrocketed in the past few years. It is predicted that over 50% of the global devices and connections will be mobile (*e.g.*, smartphones, tablets) and the monthly global mobile data traffic will surpass 30.6 exabytes ($10^{18}$) by 2020 [1]. This trend will continue in the foreseeable future.

Despite the volume of mobile cellular traffic data, we have limited knowledge on its spatio-temporal patterns at urban scale. Tremendous records of cellular traffic collected at cell towers have been widely adopted for daily network management and diagnosis. However, we argue that the big traffic data from cell towers are also beneficial to *understand* and *predict* urban cellular traffic, which can be extremely valuable for individual cell towers, cellular carriers, and city authorities. In the coming 5G era, cell towers can adapt themselves to the dynamics in traffic load based on SDN / NFV (Software-Defined Networking / Network Function Virtualization) technology. Accurate prediction of cellular traffic will facilitate carriers to schedule resources to ensure the overall quality of service and network performance and reduce unnecessary operation cost by allocating energy and bandwidth tightly based on the future traffic demand. Cellular data traffic prediction also assists city authorities to discover certain social events in time for urban governance. For instance, city managers can take prevention measures or preemptive actions for spontaneous gatherings of people to avoid injury caused by crowd stampede.

978-1-5090-6501-1/17/$31.00 

However, it is extremely challenging to predict mobile cellular traffic at both large-scale and fine granularity. The reasons are three-fold. *(i)* Due to the diverse network demand of Internet-based applications (*e.g.*, mobile videos, location-based games, VoIP) and user behaviours (*e.g.*, at work, in transit, during sleep), the cellular traffic at an individual cell tower can have a wide dynamic range. According to our dataset in a major city of China, the traffic volume can easily peak at around 1GB during rush hours (*e.g.*, 16:00), which is 100,000 times greater than the traffic during the least active times (*e.g.*, 04:00). *(ii)* User mobility introduces spatial dependencies into the cellular traffic among spatially distributed cell towers. Our dataset reveals that data traffic from mobile users (*i.e.*, entering or leaving a cell within a time interval) can account for up to 90% of the entire data traffic at cell towers in transportation hubs. We also observe that such spatial dependencies can occur even between distant cell towers, as efficient urban transportation easily enables mobile users to travel across cities within half an hour. *(iii)* Geographical distribution of cellular traffic at the urban scale is also influenced by many other factors, including land use, population, holidays, and various social activities. These influential factors further complicate the spatio-temporal dependencies among cell tower traffic citywide.

Network traffic analysis and prediction have been well studied, covering from wired Internet to cellular networks. In the past, mainstream research has modeled traffic patterns using statistics or probabilistic distribution in the time domain [2], space domain [3], or both [4]. Although these works provide a comprehensive understanding of the Internet traffic, the outcomes cannot be utilized to predict traffic load for individual cell tower continuously. Traffic prediction is more challenging than characterization. Existing solutions either totally ignore the spatial influence of cell towers at different locations [5], or use an approximate model (*e.g.*, spatial aggregation [6] [7] or statistical covariance [8]). These solutions fail to capture the intensive and often long-distance spatial dependency of individual cell towers induced by citywide user mobility, let alone the interaction between temporal and spatial factors.

In this work, we carefully investigate the characteristics of urban cellular traffic with a large-scale cellular data usage dataset covering 1.5 million users and 5,929 cell towers in a major city of China. We demonstrate that there is strong, long-distance, and pervasive spatial dependency among cell tower cellular traffic, which was overlooked in previous research. To explicitly account for the spatial dependency, we propose to decompose the total data traffic volume into in-cell traffic and inter-cell traffic, and verify the importance of such decomposition in cellular traffic prediction. We leverage a graphical representation to comprehensively capture the spatio-temporal correlations of cellular traffic, and exploit graph neural network to learn an efficient spatio-temporal model from our massive dataset. We also demonstrate that the combination of in-cell and inter-cell traffic patterns can be applied for network or social event inference, which is practically helpful for mobile carriers to adjust network configuration, or for city authorities to take preventive measures. Evaluations on our massive dataset validate the effectiveness of our graphical spatio-temporal model.

The contributions of this work are summarized as follows.

- Conceptually, we decompose cellular traffic into in-cell and inter-cell traffic to characterize the spatial dependency among cell towers, which was rarely taken into account previously. We show the necessity and benefits to account for spatial dependency in cellular traffic prediction through measurements on a massive dataset.
- We jointly consider temporal and spatial dependency among cell towers and exploit a deep neural network based model for cellular traffic prediction. The model effectively parameterizes in-cell and inter-cell traffic, and is able to learn long-distance spatial correlations for accurate traffic prediction. This is the first work that applies deep learning for individual cell tower traffic prediction at urban scale with massive real-world datasets.
- We achieve large-scale (metropolis) and fine-grained (individual cell tower, half an hour) traffic prediction and outperform the state-of-the-art by 16.3% in Mean Absolute Error (MAE) and 17.5% in Mean Absolute Relative Error (MARE). To the best of our knowledge, our work is the first that is capable of predicting in such scale and granularity and has been evaluated on a real-world big dataset.

In the rest of the paper, we describe our dataset and motivating observations in Section II and Section III, respectively. On this basis, we propose our graph-based prediction model in Section IV and evaluate the performance in Section V. Related works are reviewed in Section VI. Section VII finally concludes this study.

## II. Background and Data set

This section presents the architecture of a typical cellular network monitoring system and gives an overview of our dataset.

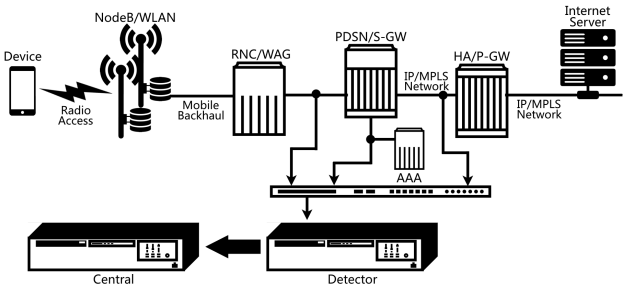


Fig. 1: An illustration of cellular network architecture and data monitoring system.

### A. Data Monitoring in Cellular Networks

Fig. 1 shows the architecture of a typical cellular network monitoring system. To facilitate network management, a monitoring system is deployed for operators to analyse data traffic, monitor network performance and detect anomalies. The monitoring system consists of a *detector* and a *central*. The detector is deployed in the packet core and the central is deployed in the Network Operations Center (NOC). Every packet sent by a mobile device will be monitored on the interface between the Packet Data Serving Node (PDSN) / Serving Gateway (S-GW) and Home Agent (HA) / Packet Data Network Gateway (P-GW) in CDMA and LTE networks. The monitoring system records important information for network diagnosis and forensics. Each record contains bidirectional flow information with the following key fields: source / destination pair by IP and / or International Mobile Station Equipment Identification (IMEI) / International Mobile Subscriber Identification (IMSI) or Network Access Identifier (NAI) / Electronic Serial Number (ESN) / Mobile Station Identifier (MSID), application(s) and wireless network resources consumed (*e.g.*, traffic volume, airtime, connection setup counts).

### B. Dataset Description

Our dataset was collected by a major cellular carrier in a big city of China. Each entry records a unique anonymized user ID, the flow create time, the flow connected cell tower ID, App ID, device type ID, uplink traffic and downlink traffic. In our study, we exploit downlink traffic for analysis. Table I summarizes the basic statistics for the dataset. To the best of our knowledge, the dataset is the one of the largest urban-scale cellular traffic dataset in terms of the number of mobile users and cell towers. The wide coverage in mobile users and cell towers promises to capture comprehensive varieties and spatial dynamics in cellular traffic patterns.

## III. Preliminary observation and Motivation

### A. Spatio-temporal Distribution of Cellular Traffic

Fig. 2 shows the spatial distribution of cellular traffic (bytes per half-hour per $km^2$) at different times (04:00, 10:00, 16:00, 00:00) on June 15th, 2016, a weekday. Specifically, cell

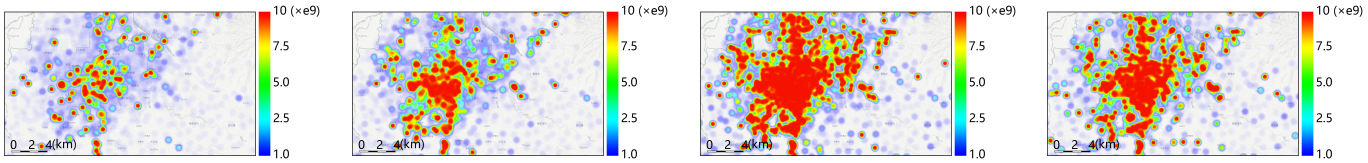


(a) 04:00 (b) 10:00 (c) 16:00 (d) 00:00

Fig. 2: Spatial distribution of urban cellular traffic at different times of a day.

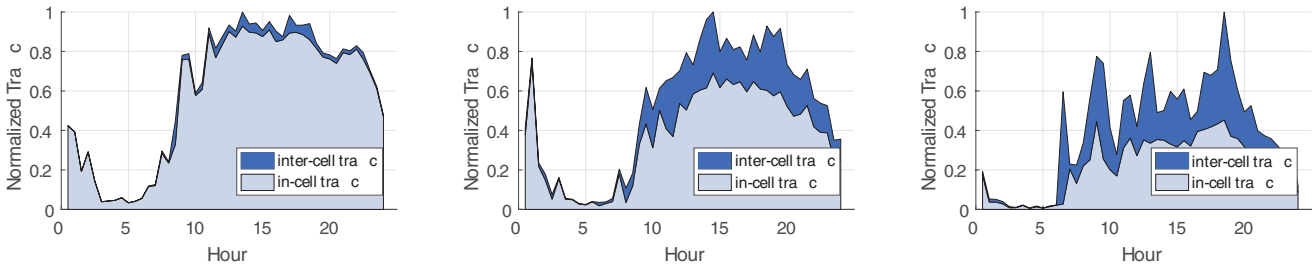


(a) (b) (c)

Fig. 3: An illustration of three typical in-cell and inter-cell cell tower data traffic characteristics. (a) In-cell traffic dominant, collected from a cell tower in a residential area; (b) Inter-cell traffic consistently notable during the daytime, collected from a cell tower in a shopping mall; (c) Inter-cell traffic surges at certain times, collected from a cell tower in a transit station.

TABLE I: Dataset Description.

| Statistics | Value |
|---|---|
| Flow Records | $1.7 \times 10^{10}$ |
| Cell Towers | $5.9 \times 10^{3}$ |
| Covered Users | $1.5 \times 10^{6}$ |
| Covered Apps | $7.0 \times 10^{2}$ |
| Covered Area | $1.0 \times 10^{4} km^2$ |
| Date | June 5th-18th, 2016 |

towers in the city center and some industry areas exhibit heavy cellular traffic throughout the day. Overall the cellular traffic before dawn (04:00) is low as most residents in the city are sleeping. At 10:00 the traffic at most areas starts to increase as most people start working. We observe intensive cellular traffic widespread through the city at 16:00, indicating people are involved in diverse activities and are highly mobile. Surprisingly, we find high volume of cellular traffic even at midnight. The reason might lie in the fact that it is a metropolis and there can be rich night life during summer.

### *B. Characterizing Cell Tower Traffic using In-cell and Inter-cell Traffic*

Existing solutions rarely consider data traffic mobility induced by human mobility, which plays a critical role in prediction according to our measurement. To understand the spatio-temporal variates of cell tower traffic, we propose to distinguish *in-cell* and *inter-cell* traffic. Specifically, instead of considering the traffic of a cell tower $c_i$ at time $t$ (denoted as $x_t(c_i)$) as a whole, we propose to decompose $x_t(c_i)$ into *in-cell traffic* $x_t^A(c_i)$ and *inter-cell traffic* $x_t^B(c_i)$, where $A$ is the set of mobile devices residing within the coverage of cell tower $c_i$, and $B$ stands for the set of mobile devices just entering the coverage of $c_i$ from another cell tower. Formally, let $P_t(c_i)$ be the set of mobile devices at cell tower $c_i$ at time $t$. Then $x_t(c_i) = x_t^A(c_i) + x_t^B(c_i)$, where $A = P_t(c_i) \cap P_{t-1}(c_i)$ and $B = P_t(c_i) \setminus P_{t-1}(c_i)$. In particular, if a mobile device traverses several cells in a unit time interval (*i.e.*, half an hour in our case), it will be associated with $c_k$ and put into the set $P(c_k)$, where $c_k$ is the last cell along its trajectory. Accordingly, its traffic during the time interval will be put on the last cell entirely. This approximation is feasible since the induced error is ignorable compared with the traffic of a cell tower.

Fig. 3 shows the normalized hourly traffic characteristics of three representative cell towers. As shown, the total traffic of all the three cell towers exhibits dramatic temporal dynamics within the day, and the three cell towers demonstrate distinctive in-cell and inter-cell traffic patterns. In the first type of cell towers (Fig. 3a), in-cell traffic overwhelms the entire cellular traffic, indicating the total traffic volume is dominated by the Internet access behaviours of a fixed group of users. In the second type of cell towers (Fig. 3b), inter-cell traffic takes up a notable portion of the total traffic in the daytime. These type of cell towers are likely to be located in places with continuous and intensive mobility in the daytime, *e.g.*, shopping malls. In the third type of cell towers (Fig. 3c), inter-cell traffic surges during the morning and evening rush hour and lunch time. A cell tower at public transportation hubs within the city may demonstrate such a traffic pattern.

Compared with the first type of cell towers, the data traffic

of the last two types of cell towers is largely determined by inter-cell traffic, which is induced by mobility. Mobility from cell to cell introduces *spatial* correlations among cell tower traffics. As a consequence, when predicting the traffic of one individual cell tower, it is important to take into account the spatial distributions and dependencies of cellular traffic of cell towers at different locations. In fact, as we will show in the evaluation, the state-of-the-art time-series based cellular traffic prediction approaches [9] [10] perform poorly for the latter two types of cell towers, as they ignore the spatial correlations among cell towers induced by mobility.

## IV. Spatio-temporal Modelling for Traffic Prediction

Motivated by the observations from the above in-cell and inter-cell traffic pattern analysis, in this section, we propose a deep graph model for fine-grained (individual cell tower, half-hour granularity) cellular traffic prediction. Furthermore, we decompose cellular traffic into explainable components and design an inference scheme to discover network or social events.

### A. Problem Statement

Formally, our cellular traffic prediction problem can be formulated as follows. Let $C = \{c_i | i = 1, \ldots, N_c\}$ denote the set of cell towers, where $c_i$ is the $i^{th}$ cell tower, and $N_c$ is the number of cell towers. Let $x_t(c_i)$ denote the traffic of a cell tower $c_i$ at time $t$. Given a set of cellular traffic $\{x_1, \ldots, x_{t-1}\}$, our goal is to predict $x_t(c)$ for all $c \in C$. As demonstrated in Section III-B, the majority of the total data traffic can be inter-cell traffic induced by mobility. Thus it is necessary and beneficial to account for spatial dependencies for accurate cellular traffic prediction. That is, we assume $x_t(c_i)$ is dependent on both $\{x_k(c_i)\}$ (temporal factor) and $\{x_k(c_j), j \neq i\}$ due to user mobility (spatial factor), where $k = 1, \ldots, t-1$.

### B. Graph Representation of Spatio-temporal Dependencies

We model the spatio-temporal dependencies of cellular traffic using a graph representation. Specifically, given a directed graph $G = (V, E)$, we denote each vertex $c \in V$ as a cell tower, and each edge $e = (c, d) \in E$ , where $d \in V$, as the spatial dependency of a cell tower $c$ on $d$. The neighbours of $c$, which have incoming edges or outgoing edges to $c$, are represented by $NBR(c)$, and $CO(c)$ stands for the edges (both incoming and outgoing) connected to $c$. Given an edge $e = (d, c) \in CO(c)$, its weight $w(e)$ is defined as the total data traffic vector of mobile devices that move from $d$ to $c$ at each time $t$, *i.e.*, $[x_1(d \to c) \cdots x_t(d \to c) \cdots]$.

Due to the large scale of our dataset (5,929 cell towers), a complete directed graph can contain huge amounts of edges (approximately 2 million), thus hindering efficient learning of model parameters. Besides, in some edges, $w(e)$ only has little number of nonzero items, which should be regarded as noise. Therefore we prune edges with small weights to speed up the learning process and empirically set a threshold of nonzero count in $w_e$ to balance prediction accuracy and computing efficiency.

One important observation in our study is that the inter-cell traffic is highly correlated with user mobility in the city. Fig. 4 shows the spatial distribution of the corresponding inter-cell traffic (per half-hour) at 04:00, 10:00, 16:00 and 00:00. The line width of each edge shows the volume of the corresponding inter-cell traffic. We omit edges of distances shorter than 3 km to investigate whether there is extensive mobility between distant cell towers.

From the figure, we find that (1) both the intensity and geographical distribution of user mobility are tightly correlated to inter-cell traffic; and (2) inter-cell traffic between two distant cell towers can be dependent because there may be intense user mobility.

The first finding justifies our decomposition of cellular traffic into in-cell traffic and inter-cell traffic to characterize spatial dependencies induced by user mobility. The second finding indicates that the spatial dependencies among cell tower traffic may not necessarily be local (*e.g.*, within the same residential district). The rapid development of urban transportation has made it easy to transit among urban transportation hubs (*e.g.*, airport, train stations), and popular locations (*e.g.*, hot tourist attractions) within half an hour. Such fast urban-scale mobility introduces enormous long-distance spatial dependency to cell towers within the whole city. Thus the neighbourhood defined in our graph representation is based on device mobility, rather than geographical distances among cell towers.

### C. Learning Spatio-temporal Dependencies via Graph Neural Networks

To efficiently learn the spatio-temporal dependency in cell tower traffic, we adopt a Graph Neural Network (GNN) [11] model. A GNN is a general neural network architecture defined on a graph structure $G = (V, E)$. Nodes $v \in V$ take unique values from $1, \ldots, |V|$ representing each cell tower in our model, and edges are pairs $e = (v, v') \in V \times V$. Since inter-cell traffic is directional, we denote $(v, v')$ as a directed edge $v \to v'$. In a GNN, each node $v$ is assigned with a hidden state named node representation, which is denoted by $h_v \in \mathbb{R}^r$, where $r$ is the dimension of node representation. Node representation $h_v$ models the spatio-temporal features for each node $v$ and is to be trained, which will be explained later.

To separately encode in-cell traffic and inter-cell traffic into a GNN, we assign in-cell traffic as the labels for each node, and inter-cell traffic as the labels of each edge. Specifically, each node $v$ is associated with a node label sequence $x^A(v) \in \mathbb{R}^l$, where $l$ is the history data length for prediction and $x^A$ is the identifier for the node labels. Similarly, each edge $e$ is associated with an edge label sequence $x^B(e) \in \mathbb{R}^l$, where $x^B$ is the identifier for the edge labels. Afterwards, it is natural to use the in-cell traffic series to represent the node sequence, *i.e.*, $x_t^A(v) = (x_{t-l}^A(v), x_{t-l+1}^A(v), \cdots, x_{t-1}^A(v))^T$, and the inter-cell traffic series to represent the edge sequence, *i.e.*, $x_t^B(e) = (x_{t-l}^B(e), x_{t-l+1}^B(e), \cdots, x_{t-1}^B(e))^T$. In the above

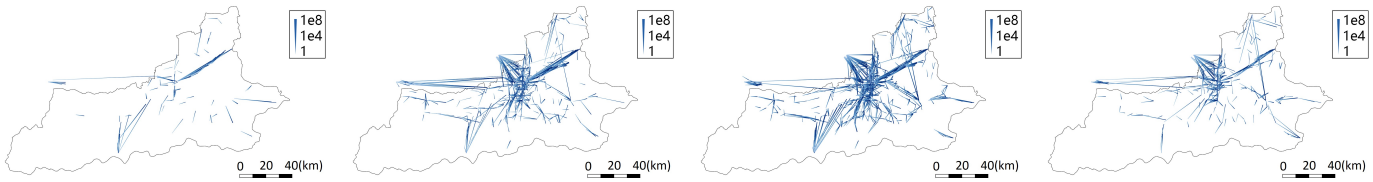


(a) 04:00 (b) 10:00 (c) 16:00 (d) 00:00

Fig. 4: Distribution of inter-cell traffic volume at different times of the same day. The line width of each edge represents the volume of inter-cell traffic between a pair of cell towers, aggregated by half an hour.

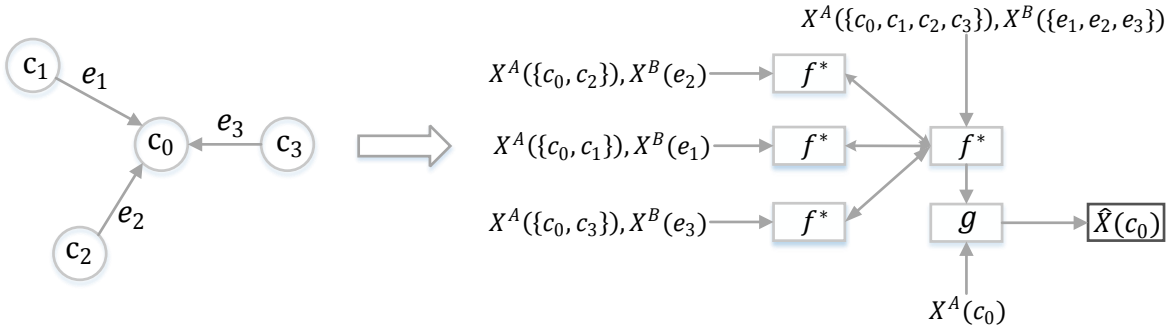


Fig. 5: An illustration of the cellular traffic prediction process for cell tower $c_0$ using GNN.

modelling, the GNN captures both temporal dependency of individual cell towers and spatio-temporal dependency among cell towers network-wide of an order of $l$, which is an important parameter for tuning.

For ease of presentation, we overload notations and let $x^A(S) = \{x^A(s)|s \in S\}, h(S) = \{h(s)|s \in S\}, x^B(S) = \{x^B(s)|s \in S\}$, and the function $In(v) = \{v'|(v',v) \in E\}$ returns the set of predecessor nodes $v'$ with $v' \to v$. Analogously, $OUT(v) = \{v'|(v,v') \in E\}$ is the set of successor nodes $v'$ with edges $v \to v'$. The set of all nodes neighbouring $v$ is $NBR(v) = IN(v) \cup OUT(v)$, and the set of all edges incoming to or outgoing from v is $CO(v) = \{(v',v'') \in E|v = v'||v = v''\}$.

A GNN model maps the graphs to the outputs (prediction of cellular traffic) in two steps: (1) a propagation step that computes the node representations $h(v)$ for each node $v$, and (2) an output model $o(v) = g(h(v), x^A(v))$ that maps the node representations (spatio-temporal features) and the corresponding node label sequence (cellular traffic history of the target cell tower) to an output $o(v)$ for each $v \in V$.

**Propagation Step**: The propagation step is an iterative procedure that propagates node representations. Initial node representations $h^{(1)}(v)$ are set to arbitrary values. Then each node representation is updated following the recurrence below until convergence, where $i$ denotes the timestep, $f^*$ denotes a function implemented by a multi-layer neural network:

$$h^{(i)}(v) = f^*\Big(x^A(v), x^A(NBR(v)), x^B(CO(v)), h^{(i-1)}(NBR(v))\Big) \quad (1)$$

**Output Model**: An output model is defined per node and is a differentiable function $o(v) = g(h(v), x^A(v))$. In our work, we adopt graph-level regression for the output model instead of mapping output $g$ for each node to emphasize the spatial dependency among cell towers. To train a GNN, all parameters (*i.e.*, node representations $h_v$ and output model $g$) are learned jointly using gradient-based optimization such as Almeida-Pineda algorithm [12] [13], which runs the propagation step to convergence and computes gradients based on the converged solution.

In this work, we train a GNN model for each cell tower. To predict $x(v)$, we feed input $x^A(v), x^A(NBR(v)), x^B(CO(v))$ into the GNN model. Since the traffic prediction model for each cell $c$ only depends on a small set of nodes and edges, the training process for all cell towers can be easily distributed and paralleled.

Fig. 5 shows an illustrative example of the GNN model we use to predict the cellular traffic for cell tower $c_0$. The figure on the left shows the graph representation of cell tower $c_0$ and its neighbours $\{c_1, c_2, c_3\}$. The in-cell traffic of each cell tower will be encoded into $c_i$ and the inter-cell traffic will be encoded into the edges $\{e_1, e_2, e_3\}$. The figure on the right describes the GNN model. Specifically, node representations $\{h(c_i)\}$, *i.e.*, the spatio-temporal features, will be learned for each cell $c_i$ in the propagation step using $f^*$ based on the in-cell traffic $X^A$ and inter-cell traffic $X^B$ of all the nodes and edges connected to $c_i$. Then the node representation $h(c_0)$, together with $X^A(c_0)$, will be fed into the output model $g$ to get the prediction result $O(c_0)$, *i.e.*, the predicted cellular traffic for $c_0$.

### D. Event Inference

In addition to data traffic prediction, the decomposition of in-cell ($x^A$) and inter-cell ($x^B$) traffic also benefits mining network (or social) events.

We decompose the cellular traffic $x$ into 3 explainable components: a seasonal component $s$ capturing the periodic pattern; a trend component $u$ capturing the offset from the periodic pattern in a period, and a residual component $r$ capturing the instantaneous changes. That is, given a prediction $x$ for cellular traffic using the GNN model, we rewrite $x = s+u+r$ with the ratio-to-moving-average method [9], and we conduct the decomposition for both the in-cell traffic and the inter-cell traffic, *i.e.*,

$$x^A = s^A + u^A + r^A$$
$$x^B = s^B + u^B + r^B$$

In particular, $r^A$ reflects the instantaneous traffic variation caused by mobility-independent online events, such as an online live show or an Internet failure, while $r^B$ corresponds to the instantaneous traffic changes caused by mobility-dependent social events, *e.g.*, a sports game, pop-music concerts, presidential campaign speech, large rallies, traffic jams, etc. Detecting such events will be beneficial for network troubleshooting and optimization as well as for urban governance and taking necessary prevention actions.

We show an example of event inference based on traffic patterns in Fig. 6. From the information of $r^A$ and $r^B$, we can observe that the traffic patterns of both $r^A$ and $r^B$ are notably different in the first two days (0-48h). On June 5th (0-24h), 2016, $r^B$ surged twice during morning and evening and the data volume reached 525% compared with normal days (the latter four days). Soon following $r^B$'s changes, $r^A$ also experienced large increases twice on June 5th, 2016, with a data traffic escalation of 3,930%. It can be observed that both $r^A$ and $r^B$ changed rapidly and it took less than half an hour from the starting to the ending of the dramatic traffic shift. This means the sampling interval of half an hour fails to capture the details of changes. This is one of the most important reasons why mobile traffic prediction is extremely challenging.

According to our previous analysis, $r^B$'s changes can be attributed to user mobility. Thus, we infer that there were people gathering at 10 a.m. and 5 p.m. and people dispersing at 1 p.m. and 9 p.m. on June 5th, 2016. On the other hand, the volume of $r^A$ shows that people accessed the Internet heavily between 10 a.m. to 1 p.m., and between 3 p.m. and 9 p.m., respectively. This observation indicates that there was either a hot online issue that many people followed through the Internet or a local event that people were willing to share on the Internet. Combining the information of both $r^A$ and $r^B$, we believe that the second possibility is more likely.

Through thoroughly search on the Internet, we find that there was a "shake run" activity with participants signing in at 12 p.m. and a concert of two pop music stars starting at 4 p.m. on June 5th. This verifies our event inference.

We believe that event inference based on traffic patterns is valuable but challenging. The difficulty lies in the lack of ground-truth information of various social events at citywide scale. The city where our dataset is collected is both an ancient and modern metropolis with a large population of more than 10 million. Numerous activities take place each day, which obstructs our search of events corresponding to traffic variation. It is common that we succeed in detecting abnormal traffic patterns but fail to verify our inference, because such activities may not be posted online, or its information hides in the ocean of Internet data and we are looking for a needle in a haystack. As a result, we are unable to conduct extensive evaluation for event inference at the current stage. However, the findings so far motivate us a lot and we will continue our exploration in this direction and leave it as a future work.

## V. Evaluation

In this section, we evaluate the performance of our spatio-temporal prediction model and compare it with the state-of-the-art time-series based prediction approaches.

### A. Experimental Settings

*1) Dataset:* We evaluate the performance of our cellular traffic prediction model on the dataset discussed in Section II-B. It covers comprehensive cellular data usage traces of 1.5 million users monitored at 5,929 cell towers from June 5th to 18th, 2016. As we aim at a temporal resolution of half an hour, we aggregate the traffic at each cell tower every half an hour. We choose data from the last two days as the testing data, and all data before that as training data.

*2) Baselines:* We compare the performance of our proposed **GNN** with **D**ecomposed Cellular Traffic model (**GNN-D**) with the following baselines.

**NAIVE** The NAIVE method simply predicts the traffic at a certain time based on the traffic at the same time of the last day. For instance, its prediction for 15:00 - 15:30, June 17th, 2016 is the traffic volume for 15:00 - 15:30, June 16th, 2016.

**ARIMA** Auto-Regressive Integrated Moving Average (ARIMA) model [9] is commonly used for modelling time series behaviours and has been widely adopted in time series prediction [14].

**LSTM** Long-Short Term Memory (LSTM) [10] is a Recurrent Neural Network (RNN) architecture. Unlike traditional RNNs, LSTM uses "gates" instead of activation functions, making it suitable to learn from experience to classify, process and predict time series when there are very long time lags of unknown sizes between important events.

**GNN-A** We apply the **GNN** model with **A**ggregated cellular traffic (**GNN-A**) as a basic GNN model. In GNN-A model, we assign the entire cellular traffic without decomposition as node labels and don't absort edge labels into the model.

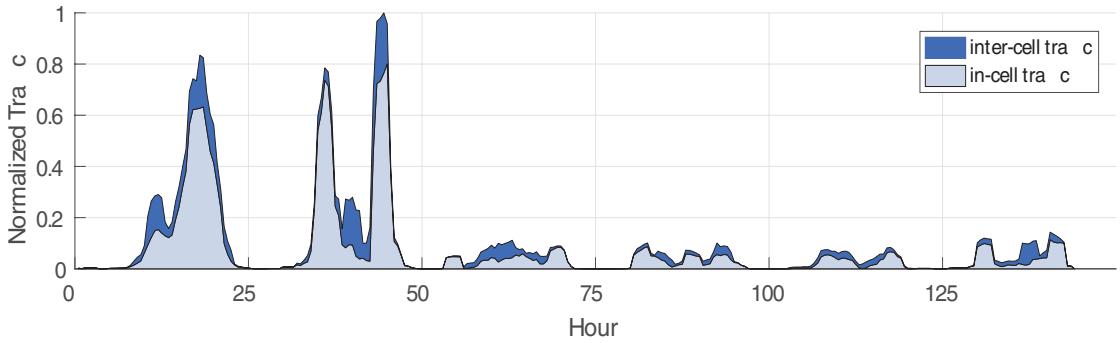


Fig. 6: An example study of cellular traffic based event inference. We detect the start of the online registration of a large activity at 12 p.m. and a people gathering event due to a concert at 4 p.m. on June 5th.

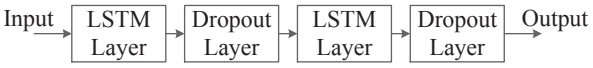


Fig. 7: Architecture of LSTM model used for evaluation.

*3) Metrics:* We evaluate the performance of cellular traffic prediction based on two metrics: Mean Absolute Error (MAE) and Mean Absolute Relative Error (MARE).

$$MAE = \frac{1}{|T| \cdot |C|} \sum_{i,j} |x_i(c_j) - \hat{x}_i(c_j)| \tag{2}$$

$$MARE = \frac{1}{|T| \cdot |C|} \sum_{i,j} \frac{|x_i(c_j) - \hat{x}_i(c_j)|}{x_i(c_j)} \tag{3}$$

where $|T|$ is the size of the testing set, $i \in [1, |T|]$ is the index of each testing sample, $j \in [1, |C|]$ is the ID of each cell, and $\hat{x}_i(c_j)$ denotes the prediction for $x_i(c_j)$.

We choose these two metrics to jointly evaluate the prediction performance of traffic volumes considering the wide dynamic range (from $10^4$ to $10^9$) of our dataset.

*4) Model Training:* We implement the ARIMA model using the "forecast" R package [15]. The package automatically selects the best model parameters based on the given order constraints. We implement the LSTM model using the "Keras" python library [16]. Fig. 7 shows the structure of the LSTM model used in our evaluation. We carefully tune the model parameters and choose 5 neurons for each LSTM layer with a 0.2 dropout rate and linear activation function, and we use the history of the last 3 time units for the best performance. We implement our GNN-A and GNN-D model using the GNN toolbox [17]. We choose two propagation layers and two output layers. Before training, features and targets will be normalized by max normalizer. We set the GNN parameters as $r = 2, l = 3$, and use 5 hidden neurons for each layer of the propagation model with *linear* activation function and 6 neurons for each layer of the output model with *tanh* activation function.

To evaluate whether our GNN model has been trained properly, we monitor the training process (1000 epochs) with qualitative metrics as shown in Fig. 8.

TABLE II: Overall prediction performance.

| Method | MAE ($\times 10^7$ bytes) | MARE |
|---|---|---|
| NAIVE | 2.784 | 1.402 |
| ARIMA | 1.309 | 2.114 |
| LSTM | 1.255 | 0.958 |
| GNN-A | 1.289 | 0.922 |
| GNN-D | 1.051 | 0.790 |

Fig. 8a plots the saturation coefficients during our training. Saturation coefficient is defined as the mean square error of the hidden layer's output in our experiment. For tanh layers, a hidden unit is saturated if the saturation coefficient is close to 1 or $-1$. For linear models, certain degree of saturation is essential, while for non-linear models, saturated layer will decrease both the information capacity and the learning ability of a neural network [18]. We monitor the saturation coefficients for both the propagation step (denoted as "propagationNet", linear) and for the output model (denoted as "outputNet", non-linear). As shown, the saturation coefficients for the propagationNet and the outputNet are both in the range $(0.01, 0.05)$, indicating the training process is nonmalignant.

Fig. 8b shows the stability coefficients during the training process. Stability coefficient measures the difference of outputs between successive epochs, *i.e.*, $\frac{\sum |(o^{(t)} - o^{(t-1)}|}{\sum |o^{(t)}|}$, and indicates whether the training converges. As shown, the stability coefficient gradually drops to nearly zero after 400 epochs, indicating that the training process will converge.

Fig. 8c shows the normalized mean squared errors (Normalized MSE) on traffic prediction using the validation set. As shown, after about 80 epochs, both the learning error and the validation error converge, demonstrating the effectiveness of the training process.

### B. Prediction Performance

Table II summarizes the traffic prediction performance of our GNN-D methods and the baselines. GNN-D consistently and significantly outperforms all the baselines in both metrics. Specifically, GNN-D achieves 62.2%, 19.7%, 16.3%, 18.5% smaller MAE than NAIVE, ARIMA, LSTM and GNN-A, respectively, and demonstrates 43.7%, 62.6%, 17.5%, 14.3%

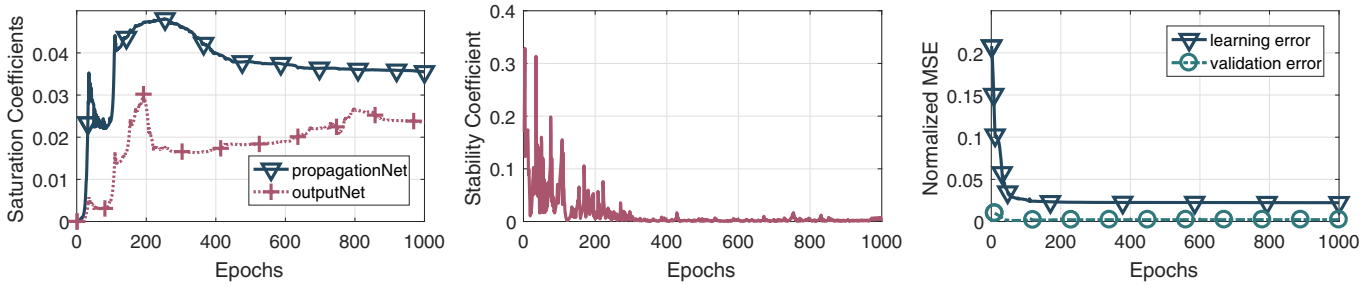


(a) (b) (c)

Fig. 8: Quantitative monitoring of the training process in 1000 epochs. (a) Satiation coefficients of the models in both propagation and output steps. (b) Stability coefficient and (c) Normalized MSE showing the convergence of training.

improvement in MARE than NAIVE, ARIMA, LSTM and GNN-A, respectively.

For more insights on the applicability of our method, we investigate the impact of different factors on the cellular traffic prediction performance as follows.

**Impact of Cellular Traffic Volume.** To evaluate the prediction performance for different traffic volume, we divide the testing set into four subsets based on traffic volume levels: $[0, 10^6), [10^6, 10^7), [10^7, 10^8), [10^8, +\infty]$.

Fig. 9(a) and Fig. 9(b) present the prediction performance for different traffic volume levels. We make the following observations from the results. *(i)* For all prediction methods, MAE increases with the traffic volume while MAPE decreases with the traffic volume. *(ii)* GNN-A performs similarly to LSTM. It could be explained that the propagation model in GNN-A is equivalent to a basic recurrent neural network. Without traffic decomposition, the neural network has similar encoding capacity for spatial time series to LSTM. *(iii)* GNN-D method outperforms the baselines in all levels of traffic volume. The results indicate that even with an imbalanced training dataset, our method still outperforms others in predicting extremely light or heavy traffic and it is applicable to traffic volumes spanning a wide dynamic range.

**Impact of Spatial Dependency.** This experiment demonstrates the prediction performance of our method for cell tower traffic with different levels of spatial dependency. We quantify the spatial dependency of cell towers using centrality, which is a graph term to measure the importance of vertices. There are various ways to define centrality such as closeness centrality, betweenness centrality, Eigenvector centrality and PageRank centrality [19]. PageRank centrality measures centrality by considering three distinct factors: *(i)* the number of links it receives, *(ii)* the link propensity of the linkers, and *(iii)* the centrality of the linkers. Thus PageRank centrality is the most suitable to measure the levels of spatial dependency of each cell tower. Fig. 10 shows the distribution of PageRank centrality in the main district of the city where our measurements were collected. Each point represents a cell tower and its color stands for the value of its PageRank centrality. We select three cell towers with high PageRank centrality, denoted by 'A', 'B' and 'C' in Fig. 10. After checking the city maps, we find that cell tower A is located at a railway station, cell tower B is within a major shopping mall, and cell tower C is in a university. All of them are busy and crowded locations with high user mobility. In all of the three cell towers, inter-cell traffic takes up a large portion of the total traffic volume and we expect high spatial dependency of their cellular traffic on the neighbouring cell towers.

After showing that PageRank centrality can act as an indicator for spatial dependency of cellular traffic, we plot the prediction performance of our method for cell towers within different PageRank centrality levels in Fig. 9(c) and Fig. 9(d). As shown, with the increase of PageRank centrality (and thus spatial dependency), MAE increases slightly while MAPE decreases significantly for all the prediction schemes. Considering that cells with high spatial dependency usually have high traffic volume, the slightly increased MAE in fact leads us to conclude that our method is more accurate for highly spatial-dependent cells. And GNN-D consistently outperforms the baselines. For instance, for cell towers with high centrality ($\geq 1.2 \times 10^{-2}$), GNN-D is 23.3%, 20.5%, 19.0% better than ARIMA, LSTM and GNN-A in MAE, and 60.7%, 26.2%, 11.2% better than ARIMA, LSTM and GNN-A in MARE.

**Temporal View of Prediction Errors.** This experiment shows the temporal trend of the prediction errors of all the methods. Since both the traffic volume and its changing rate usually vary with time, the experiment demonstrates how the prediction accuracy is affected by traffic volume and traffic changing rate. Fig. 9(e) and Fig. 9(f) plot the MAE and MARE metrics during one day. In accord with our evaluations of the impact of traffic volume on the prediction performance, during busy hours in the morning (7:00, 9:00, 11:00), MAE increases while MARE decreases, as the traffic peaks at these times. One exception is that at 10:00, there is a valley in cellular traffic, and it is expected that for all the methods, MAE will decrease and MARE will increase. However, both ARIMA and LSTM have large MAE, indicating that they fail to predict even modest traffic volume. A closer look at the traffic pattern around 10:00 shows that the cellular traffic changes rapidly around 10:00, suggesting intensive mobility, and thus strong mobility. As ARIMA, LSTM and GNN-A fail to account for

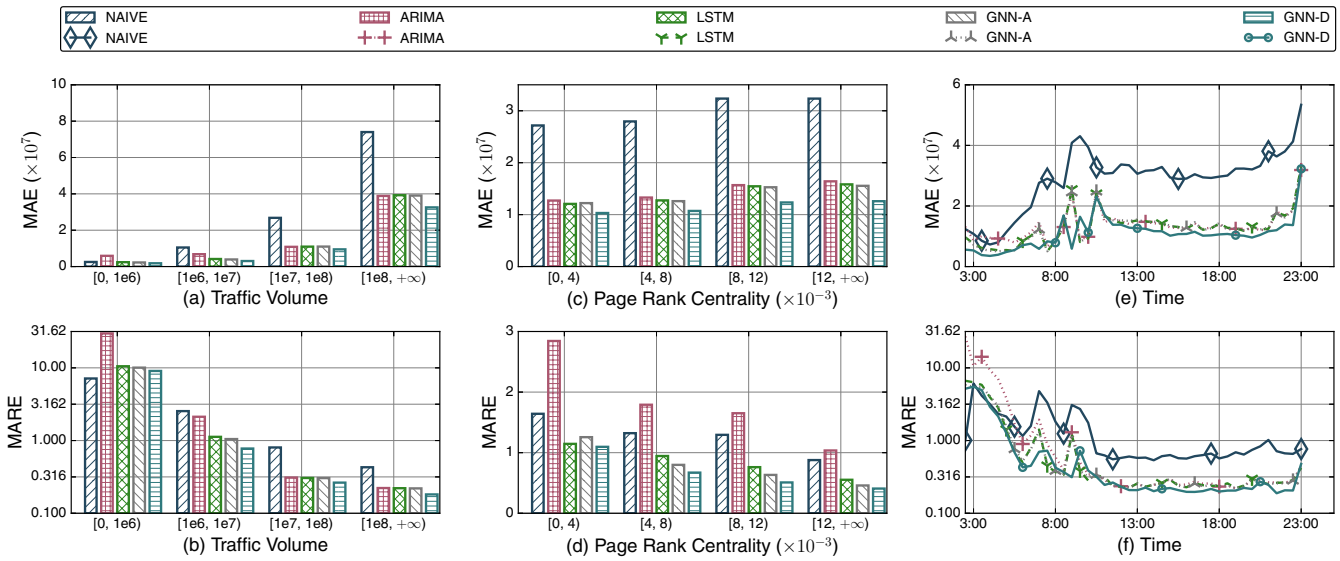


Fig. 9: Different perspectives on predicting performance.

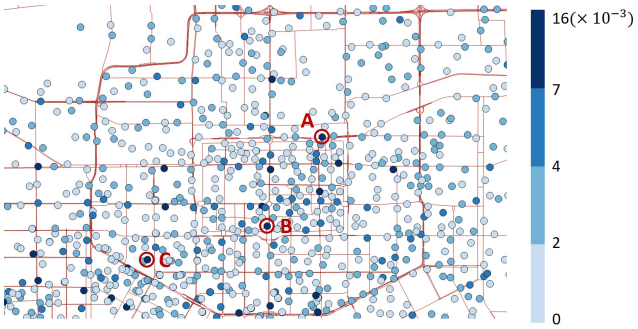


Fig. 10: Spatial distribution of PageRank centrality.

spatial dependency of cellular traffic, they naturally perform poorly when there is intensive mobility. In contrast, GNN-D encodes the spatial dependency into the graph model, so that it can still predict the fast-changing cellular traffic accurately and achieve small MAE.

## VI. Related Work

Network traffic analysis and prediction has a long history, from the emergence of data network several decades ago to today, spanning from Internet [20] [21] to cellular networks (*e.g.*, voice call [22] and SMS [23]).

In recent years, the explosive growth of mobile Internet applications has drawn numerous research attempts to characterize cellular traffic from both academy and industry. Network traffic prediction could benefit plenty of applications. According to the sources of data traffic records, existing works can be generally divided into two categories: *(i)* data recorded by mobile devices; *(ii)* traces collected by cellular operators. For the first category, phone usage information, including locations, applications, network performance, is automatically monitored and logged by mobile APPs [24] [25], some of which work in a crowdsensing manner [26], [27]. The major limitation of this approach lies in its scale; that is, the user coverage of data traces is restricted within a group of people who install some specific APPs on their mobile devices. As a result, the statistics obtained cannot truly reflect the whole set of users associated with a cellular tower, not to mention the global characteristics of a large scale cellular network. On the other hand, in the dataset collected by cellular operators, users are passively monitored without awareness. In fact, mobile carriers are able to record a wealth of information in many aspects [28] [29], depending on where and in which layer the monitors are placed in cellular networks. Datasets of the second category are often employed for analyzing network-wide statistics with a large user population. Our work, relying on the dataset collected from citywide cell towers, falls into the second category.

Most previous works on cellular traffic focus on how to characterize and understand their statistics and patterns under the circumstance of various temporal and spatial factors, device types, application categories, user groups, etc. From the time domain, the traffic dynamics of IP traffic can be well captured by Markov models [2]. An interesting fact from [30] is that only five basic temporal patterns of traffic exist among cell towers in a city and each of the pattern maps to one type of geographical locations related to urban ecology. This branch of researches focuses mostly on temporal variations without spatial relationship of cells at different locations. From the space domain, Gotzner et al. [3] breach the homogeneous assumption in regular spectrum frequency analysis and propose to model the spatial inhomogeneity of real cellular traffic with log-normal distributions. [5] demonstrates that the spatial distribution of the traffic density can be approximated by the log-normal or Weibull distribution. Furthermore, [4] finds that the mobile traffic loads follow a trimodal distribution, which is the combination of compound-exponential, power-

law and exponential distributions, in terms of both spatial and temporal dimension. These approaches provide comprehensive understanding of cellular traffic, *e.g.*, temporal dynamics and spatial inhomogeneity. However, it still has a long away to realize traffic prediction.

For the more challenging problem of prediction, by treating data traffic of cell towers as a time series, the mainstream solutions employ time domain data analysis and modeling, such as AutoRegressive Integrated Moving Average (ARIMA) and Holt-Winters method [31], stochastic process models, Kalman filtering, etc.

Applying statistical covariance functions, a recent work [8] considers temporal and spatial factors simultaneously, which is the most similar to our work. However, the traffic transfer among cell towers caused by human mobility is not taken into account. Another attempt [6] models the spatial correlation by clustering nearby cell towers with the same traffic pattern into groups and predicts aggregated traffic for each group. Such relaxation in space domain neither captures spatial correlation of faraway cell towers, nor provides useful results for individual cell tower. We adopt an upgraded version of [6] as the state of the art comparison in our evaluation, via replacing Elman neural network used in [6] with an up-to-date Long short-term memory (LSTM) neural network. Different from these two similar works, our proposed solution explicitly models spatio-temporal dependency from inter-cell and in-cell traffic and predicts cellular traffic at a large scale and fine granularity, through a neural network that can learn from a graph structure.

## VII. Conclusion

Motivated by the decomposition of in-cell and inter-cell data traffic, we model the spatio-temporal features of traffic patterns in a metropolis by a directed graph and propose a powerful deep learning approach that can learn from a graph structure. We achieve large-scale and fine-grained prediction based on a big data set of cellular network records collected by a mobile carrier.

Experiment results show that the spatial dependency and the interaction of spatial and temporal factors play an important role in accurate and robust prediction. Our findings also include how their interaction can be used for event inference through example study. In the future, along with the explosive growth of mobile Internet and continuously evolving traffic patterns, known models are outdated and new opportunities are sprouting.

## VIII. Acknowledgement

This work is supported in part by the NSFC under grant 61522110, 61332004, 61572366, 61602381, Beijing Nova Program under grant Z151100000315090.

## References

[1] C. V. N. I. Cisco, "Global mobile data traffic forecast update, 2015–2020 white paper," 2016.

[2] M. Z. Shafiq and L. e. Ji, "Characterizing and modeling internet traffic dynamics of cellular devices," in *Proc. SIGMETRICS*. ACM, 2011, pp. 305–316.

[3] U. Gotzner and R. Rathgeber, "Spatial traffic distribution in cellular networks," in *Proc. VTC*, vol. 3. IEEE, 1998, pp. 1994–1998.

[4] H. Wang and J. e. Ding, "Characterizing the spatio-temporal inhomogeneity of mobile traffic in large-scale cellular data networks," in *Proc. HotPOST*. ACM, 2015, pp. 19–24.

[5] D. e. Lee, "Spatial modeling of the traffic density in cellular networks," *IEEE Wireless Communications*, vol. 21, no. 1, pp. 80–88, 2014.

[6] Y. Zang, F. Ni, Z. Feng, S. Cui, and Z. Ding, "Wavelet transform processing for cellular traffic prediction in machine learning networks," in *Proc. ChinaSIP*. IEEE, 2015, pp. 458–462.

[7] J. Wang and T. J. *et al.*, "Spatiotemporal modeling and prediction in cellular networks: A big data enabled deep learning approach," in *Proc. INFOCOM*, vol. 3. IEEE, 2017, pp. 1323–1331.

[8] X. Chen, Y. Jin, S. Qiang, W. Hu, and K. Jiang, "Analyzing and modeling spatio-temporal dependence of cellular traffic at city scale," in *Proc. ICC*. IEEE, 2015, pp. 3585–3591.

[9] G. E. Box, G. M. Jenkins, G. C. Reinsel, and G. M. Ljung, *Time series analysis: forecasting and control*. John Wiley & Sons, 2015.

[10] S. Hochreiter and J. Schmidhuber, "Long short-term memory," *Neural computation*, vol. 9, no. 8, pp. 1735–1780, 1997.

[11] F. Scarselli and G. *et al.*, "The graph neural network model," *IEEE Transactions on Neural Networks*, vol. 20, no. 1, pp. 61–80, 2009.

[12] L. B. Almeida, "A learning rule for asynchronous perceptrons with feedback in a combinatorial environment," in *Artificial neural networks*. IEEE Press, 1990, pp. 102–111.

[13] F. J. Pineda, "Generalization of back-propagation to recurrent neural networks," *Physical review letters*, vol. 59, no. 19, p. 2229, 1987.

[14] J. D. Hamilton, *Time series analysis*. Princeton university press Princeton, 1994, vol. 2.

[15] R. J. Hyndman and Y. Khandakar, "Automatic time series forecasting: the forecast package for R," *Journal of Statistical Software*, vol. 26, no. 3, pp. 1–22, 2008.

[16] F. Chollet, "Keras," https://github.com/fchollet/keras, 2015.

[17] W. Uwents, G. Monfardini, H. Blockeel, M. Gori, and F. Scarselli, "Neural networks for relational learning: an experimental comparison," *Machine Learning*, vol. 82, no. 3, pp. 315–349, 2011.

[18] A. Rakitianskaia and A. Engelbrecht, "Measuring saturation in neural networks," in *Proc. SSCI*. IEEE, 2015, pp. 1423–1430.

[19] P. Bonacich, "Power and centrality: A family of measures," *American journal of sociology*, vol. 92, no. 5, pp. 1170–1182, 1987.

[20] P. Gill, M. Arlitt, Z. Li, and A. Mahanti, "Youtube traffic characterization: a view from the edge," in *Proc. IMC*. ACM, 2007, pp. 15–28.

[21] J. Cao and W. S. e. Cleveland, "Stochastic models for generating synthetic http source traffic," in *Proc. INFOCOM*, vol. 3. IEEE, 2004, pp. 1546–1557.

[22] D. Willkomm and M. *et al.*, "Primary users in cellular networks: A large-scale measurement study," in *Proc. DySPAN*. IEEE, 2008, pp. 1–11.

[23] P. Zerfos, X. Meng, S. H. Wong, V. Samanta, and S. Lu, "A study of the short message service of a nationwide cellular network," in *Proc. IMC*. ACM, 2006, pp. 263–268.

[24] A. Noulas and M. *et al.*, "Exploiting foursquare and cellular data to infer user activity in urban environments," in *Proc. MDM*, vol. 1. IEEE, 2013, pp. 167–176.

[25] Y. Li and C. e. Peng, "Mobileinsight: Extracting and analyzing cellular network information on smartphones," in *Proc. MobiCom*, 2016.

[26] B. Guo, Q. Han, H. Chen, L. Shangguan, Z. Zhou, and Z. Yu, "The emergence of visual crowdsensing: Challenges and opportunities," *IEEE Communications Surveys & Tutorials*, 2017.

[27] X. Zhang, Z. Yang, W. Sun, Y. Liu, S. Tang, K. Xing, and X. Mao, "Incentives for mobile crowd sensing: A survey," *IEEE Communications Surveys & Tutorials*, vol. 18, no. 1, pp. 54–67, 2016.

[28] Y. Jin and N. e. Duffield, "Characterizing data usage patterns in a large cellular network," in *Proc. CellNet*. ACM, 2012, pp. 7–12.

[29] Y. Zhang and A. Årvidsson, "Understanding the characteristics of cellular data traffic," *ACM SIGCOMM Computer Communication Review*, vol. 42, no. 4, pp. 461–466, 2012.

[30] H. Wang, F. Xu, Y. Li, P. Zhang, and D. Jin, "Understanding mobile traffic patterns of large scale cellular towers in urban environment," in *Proc. IMC*. ACM, 2015, pp. 225–238.

[31] V. Sciancalepore and K. e. Samdanis, "Mobile traffic forecasting for maximizing 5g network slicing resource utilization," in *Proc. INFOCOM*, vol. 3. IEEE, 2017, pp. 2583–2591.